

Shear yielding of amorphous glassy solids: Effect of temperature and strain rate

Jörg Rottler*[†] and Mark O. Robbins

*Department of Physics and Astronomy, The Johns Hopkins University,
3400 N. Charles Street, Baltimore, Maryland 21218*

(Dated: October 2, 2018)

We study shear yielding and steady state flow of glassy materials with molecular dynamics simulations of two standard models: amorphous polymers and bidisperse Lennard-Jones glasses. For a fixed strain rate, the maximum shear yield stress and the steady state flow stress in simple shear both drop linearly with increasing temperature. The dependence on strain rate can be described by either a logarithm or a power-law added to a constant. In marked contrast to predictions of traditional thermal activation models, the rate dependence is nearly independent of temperature. The relation to more recent models of plastic deformation and glassy rheology is discussed, and the dynamics of particles and stress in small regions is examined in light of these findings.

PACS numbers: 83.60.La, 83.10.Rs, 64.70.Pf

I. INTRODUCTION

Deformation processes and plasticity in amorphous materials such as metallic or polymeric glasses have recently received a lot of attention [1, 2, 3, 4, 5]. These materials are used in many load-bearing applications. However, an understanding of their yield and flow properties is hampered by the absence of long-range order and easily identifiable mechanisms that mediate the deformation such as dislocation motion in crystals. A similar situation is encountered in “soft” glassy materials such as foams, pastes, and colloidal suspensions, which are also characterised by a liquid-like structure and long relaxation times. In fact, it has been suggested recently that these very different materials can be viewed as particular realizations of a jammed state [6], which implies that their mechanical behavior could be described in a common framework.

Much insight into the mechanical behavior of structural glasses has been gained from molecular simulations of simple glass-forming liquids or polymers, where particles interact through a Lennard-Jones potential. For example, Falk and Langer [3] studied two-dimensional shear deformation of a mixture of such particles and found localization of plastic events in so-called shear transformation zones. Barrat and Berthier [7] studied the steady state flow of a similar model and analyzed its relation to the fluctuation-dissipation theorem in out-of-equilibrium situations.

In a recent paper [2], we have studied the onset of shear yielding of amorphous polymer glasses under multiaxial loading conditions. A pressure-modified von Mises criterion [8] accurately describes the maximum shear yield stress as a function of the applied stress for different temperatures. However, in these simulations the bulk

polymer was deformed at a single constant strain rate. The present work investigates the effect of strain rate on the stress at the onset of shear yielding as well as on the steady state flow stress of glassy materials in simple shear. In order to relate the onset of yield to steady shear, we not only discuss the macroscopic material response, but also perform an analysis of the localized dynamics of the stress distribution in the deforming solid. Such a program is particularly suited to test predictions of models of plasticity [3, 4, 9, 10, 11] and may lead to a deeper understanding of the nature of plastic deformation.

In the following section, we briefly summarize traditional and more recent models of viscoplasticity and rheology of glassy materials. Sections III and IV discuss the molecular models and the simulation results, respectively. Section V critically reviews how the theoretical ideas of Section II describe the simulation results.

II. MODELS OF PLASTICITY AND RHEOLOGY

A. Rate and temperature dependence: Eyring model

The simplest model that makes a prediction for the rate and temperature dependence of shear yielding is the rate-state Eyring model [1, 9] of stress-biased thermal activation. Structural rearrangement is associated with a single energy barrier E that is lowered or increased linearly by an applied stress σ . This defines transition rates of the form

$$R_{\pm} = \nu_0 \exp \left[-\frac{E}{k_B T} \right] \exp \left[\pm \frac{\sigma V^*}{k_B T} \right], \quad (1)$$

where ν_0 is an attempt frequency and V^* is a constant called the “activation volume.” In glasses, the transition rates are negligible at zero stress. Thus at finite stress one needs to consider only the rate R_+ of transitions in the direction aided by stress. The plastic strain rate $\dot{\epsilon}_{pl}$ will be proportional to R_+ , $\dot{\epsilon}_{pl} = cR_+$. Solving for the

*present address: Laboratoire de Physico-Chimie Théorique, ESPCI, 10 rue Vauquelin, F-75231 Paris Cedex 05, France

[†]Electronic address: Joerg.Rottler@jhu.edu

stress σ , one obtains

$$\sigma = \frac{E}{V^*} + \frac{k_B T}{V^*} \ln \left[\frac{\dot{\epsilon}_{pl}}{cV_0} \right]. \quad (2)$$

Eq. (2) contains only a single relaxation time scale and predicts an apparent yield stress that varies logarithmically with the strain rate and a prefactor that depends linearly on temperature. Despite its simplicity, experimental results [8] are often fitted to Eq. (2), and the value of V^* is associated with a typical volume required for a molecular shear rearrangement.

B. Modern approaches

Modern phenomenological approaches pay tribute to the complexity of glassy systems through several extensions. First, it has been realized that assuming a single energy barrier for rearrangements is an oversimplified description of glassy materials [5]. One can therefore introduce a distribution of barriers and add additional time scales. Second, any theory that attempts to predict a full stress-strain curve must contain some information about the internal state of the system as a function of time or strain. Extensions therefore consider dynamical internal state variables. In the following, we describe particular realizations of these ideas.

1. Shear transformation zone theory

Falk and Langer used molecular dynamics simulations very similar to the present study to identify local plastic rearrangements under shear. They formulated a theory of viscoplasticity [3] based on the concept of “shear transformation zones” (STZ), bistable (mesoscopic) regions that transform under shear between \pm -states. One then considers the dynamics of an ensemble of STZ with number density n_{\pm} on a mean-field level, which determines the plastic strain rate

$$\dot{\epsilon}_{pl} = A_0(R_+n_+ - R_-n_-), \quad (3)$$

where A_0 is a constant. A key difference from the Eyring model resides in the form of the transition rates R_{\pm} , which are assumed to be free-volume (entropically) activated rather than thermally activated, i.e.

$$R_{\pm} = R_0 \exp \left[-\frac{v_0 \exp[\mp\sigma/\bar{\mu}]}{v_f} \right], \quad (4)$$

where v_0 is a characteristic free volume required for a STZ flip and $\bar{\mu}$ a characteristic stress scale required for a molecular rearrangement. The role of temperature is played by a “free volume” v_f per particle. The authors motivate this with the observation that in a solid at very low temperature, energy barriers should be very large compared to thermal energies and thus, as in granular

systems, thermal activation over these barriers should be negligible. The population densities themselves evolve according to the rate equation

$$\dot{n}_{\pm} = R_{\mp}n_{\mp} - R_{\pm}n_{\pm} + \sigma\dot{\epsilon}_{pl}(A_c - A_a n_{\pm}), \quad (5)$$

where the last term introduces creation and annihilation processes of STZ’s proportional to the work of plastic deformation $\sigma\dot{\epsilon}_{pl}$. The STZ equations can be solved analytically in special steady state situations and otherwise solved numerically. They were shown [3] to have both a jammed solution for which $\dot{\epsilon}_{pl} = 0$ and a flowing solution once σ exceeds a true yield stress σ_y . The shear rate rises linearly as sigma increases above σ_y as in a Bingham fluid. Numerical stress-strain curves, hysteresis experiments and creep tests were shown to be accurately reproduced by the model after the adjustment of several fit parameters.

Lemaître [4] recently extended STZ theory with concepts from the physics of granular media. He treated the free volume parameter v_f as a dynamical state variable and proposed the following time evolution:

$$\dot{v}_f = -R_1 \exp \left[-\frac{v_1}{v_f} \right] + A_v \sigma \dot{\epsilon}_{pl}. \quad (6)$$

This expression is motivated by slow density relaxations in granular materials that decrease the free volume. The activation factor $\exp[-v_1/v_f]$ describes the probability for volume fluctuations larger than a characteristic volume v_1 . Note that the “activation barrier” for compaction v_1 differs *a priori* from the barrier for shear transformation v_0 . The second term refers to creation of free volume (shear induced dilatancy) again due to plastic deformation. A “linearized” version of this theory produces a power law relation between shear rate and shear stress, $\sigma \sim \dot{\epsilon}_{pl}^{\kappa-1/\kappa+1}$, where $\kappa = v_1/v_0$. The full theory can yield more complicated functional forms with a true yield stress [4].

2. Soft Glassy Rheology model

The soft glassy rheology (SGR) model of Sollich *et al.* [10] is an extension of a trap model for glasses originally proposed by J.-P. Bouchaud [12] with stress acting as an external drive. It was designed to describe the flow behavior of foams, dense emulsions, pastes and slurries. However, it is very similar to the previous models and should also be relevant to the materials of interest here. Small volume elements are assumed to yield with a rate $\Gamma_0 \exp[-(E - kl^2/2)/x]$, where l is the local strain and k an elastic constant. The role of temperature is replaced by a “noise” temperature x , which is assumed to describe the effect of structural rearrangements in a mean-field spirit. Note that the model describes stress-assisted yielding as in the other two models, but stress enters quadratically and not linearly. Structural disorder is modeled with an exponential distribution of yield

energies E , $\rho(E) = \exp(-E/x_g)/x_g$, where x_g is usually set to one. This introduces a distribution of relaxation timescales. After yielding of a volume element, a new yield energy is drawn from $\rho(E)$ and the local strain l rises again from 0 according to a macroscopic shear rate $\dot{\gamma}$. The time evolution of the probability $P(l, E; t)$ describing the ensemble of volume elements can be obtained from a master equation.

Like the STZ theory, the predictions arising from the SGR equations are richer than the simple Eyring model. The exponential distribution of traps induces a dynamical glass transition, and the system exhibits aging for $x < 1$. Analysis has mainly focused on the steady state situation under constant shear rate $\dot{\gamma}$, which is the generic experiment used to determine the mechanical properties of soft glassy materials. Salient predictions are: a Newtonian fluid flow $\sigma \propto \dot{\gamma}$ for $x > 2$ and a power law fluid $\sigma \propto \dot{\gamma}^{x-1}$ for $1 < x < 2$ [10]. In the glassy phase, a scaling of the form $\sigma - \sigma_y \propto \dot{\gamma}^{1-x}$ is predicted. The nature of the noise temperature x (not the true thermodynamic temperature) and the pre-exponential factor Γ_0 (thermal) remain largely unspecified.

3. Microscopic Approaches

The descriptions of nonlinear rheology and plasticity described so far are appealing because of their simplicity, but much of the physics is put in “by hand”. In the most recent literature, efforts are made to derive the response of driven glassy systems from microscopic considerations. Berthier *et al.* [11] consider a generic driven glassy system by calculating the correlation and response functions from the microscopic Langevin equations in a mean-field approximation. Based on this approach, they suggest a “two-time-scale scenario,” in which the slow time scales associated with structural relaxations are accelerated by the drive, while the fast degrees of freedom (phonons) remain at the thermodynamic temperature. This concept can be extended to introduce an “effective temperature” different from the thermodynamic temperature. A relevant conclusion for the present work is that in their calculations for $T > T_c$ [13], the slow relaxation time t_α decreases with the drive, $t_\alpha \sim \dot{\gamma}^{-2/3}$. Since the relaxation time determines the viscosity, this leads to power law shear thinning, $\sigma \sim \dot{\gamma}^n$ with exponent $n = 1/3$. Below T_c , their numerical results indicate that n is only very weakly temperature dependent.

III. MOLECULAR SIMULATIONS

We perform three-dimensional molecular dynamics (MD) simulations for two model glasses. A bead-spring model is used for polymers. Beads of mass m interact via a conventional 6-12 Lennard-Jones (LJ) potential. All results will be expressed in terms of the characteristic length a , energy u_0 and time $\tau_{LJ} = \sqrt{ma^2/u_0}$ of this

potential. Unless otherwise noted, the potential is truncated at $r = r_c = 1.5a$ for computational convenience. We construct linear polymer chains by connecting adjacent beads with the finite extensible nonlinear elastic (FENE) bond potential [14]. This polymer model has been used extensively to study polymer melt dynamics [15] and was also used in our previous study of yield conditions [2]. The number of beads per chain used below is usually 256, but the chain length and entanglement effects are not important for the small strains considered in Section IV A.

In addition to the polymer, a binary mixture composed of 80% A-particles and 20% B-particles without covalent bonds is also studied. LJ interaction parameters were set to the values employed in previous studies that aimed at verifying predictions of mode-coupling theory for supercooled liquids [16], and studied aging [17] or dynamical heterogeneities [18] during the glass transition. A very similar system with slightly different parameters was used by Falk [3] to study deformation and plasticity in amorphous metals in two dimensions.

Both the polymer and binary mixture models enter an amorphous glassy state without crystallization upon cooling. For the polymer model, the glass transition temperature $T_g \approx 0.35 \pm 0.05u_0/k_B$, while T_g is smaller for the binary system. These values are for $r_c = 1.5a$, and slightly higher values of T_g are obtained with larger r_c [19]. Here, we focus on a temperature range between $T = 0.01u_0/k_B$ and $T = 0.3u_0/k_B$. Unless noted, the temperature is controlled with a Langevin thermostat (damping rate $1\tau_{LJ}^{-1}$). The equations of motion are solved using the velocity Verlet algorithm with a timestep of $dt = 0.0075 \tau_{LJ}$.

The simulation cell contained 32768 LJ beads. Previous studies of the yield behavior [2] have shown that an increase of the system size beyond this size leads to slightly lower values of the shear yield stress, but the generic behavior is unchanged. In order to minimize statistical fluctuations while varying the strain rate, we use the same initial state for all runs at a given temperature. The glassy states were prepared by a quench from a fluid temperature of $T = 1.3u_0/k_B$ to a glassy temperature of $T = 0.3u_0/k_B$ at constant volume over a time interval of order $1000\tau_{LJ}$. The density was chosen so that the hydrostatic pressure was zero at this temperature. Lower temperatures were then reached by cooling at constant pressure.

In studies of initial yield behavior, periodic boundary conditions are applied in all directions to eliminate edge effects. The original cell is cubic and at zero hydrostatic pressure. Tensile or compressive strains are imposed on one or more axes by rescaling the periods L_i . We use true strain rates $\dot{\epsilon}_i = L_i^{-1}dL_i/dt$ between $\dot{\epsilon}_i = 10^{-6} \tau_{LJ}^{-1}$ and $\dot{\epsilon}_i = 10^{-3} \tau_{LJ}^{-1}$. Note that since $\tau_{LJ} \sim 3$ ps, the strain rates employed are much higher than typical experimental strain rates. As discussed below, sound propagation is too slow for stress to equilibrate across the system at the highest strain rates. However, most simulations are

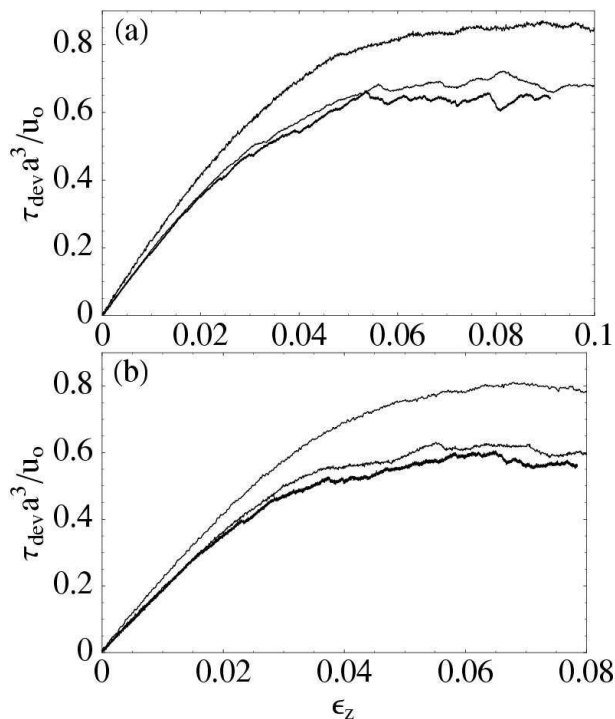


FIG. 1: Stress-strain curves for (a) the polymer glass and (b) the 80/20 LJ glass at $T = 0.01u_0/k_B$ and three different strain rates $10^{-3}\tau_{\text{LJ}}^{-1}$, $10^{-4}\tau_{\text{LJ}}^{-1}$, and $10^{-5}\tau_{\text{LJ}}^{-1}$ (from highest to lowest curves).

slow enough that loading proceeds nearly quasistatically.

Steady state flow cannot be investigated by deforming the simulation box in the above manner, because some box periods would soon decrease to a single molecular diameter. One approach is to use Lees-Edwards boundary conditions [20]. Here, we choose a different route and replace the periodic boundary conditions in the 3-direction with two rigid walls composed of 2 layers of an fcc(111) crystal for simulations of simple shear. Otherwise, the simulation cell has the same dimensions and size, and the wall beads are strongly coupled to the sheared glass so that slip at the interface is prohibited. By moving one wall parallel to the solid at constant velocity v_x , a steady state shear profile is imposed, and we can measure the shear stress τ as a function of the average strain $\gamma = tv_x/h$, where $h = 32a$ is the wall separation and t is the elapsed time. In these simulations, the Langevin thermostat is only coupled to the irrelevant (y) direction perpendicular to the flow (x) and velocity gradient (z) directions [21].

IV. RESULTS

A. Onset of shear

In ref. [2] we analyzed the onset of shear deformation in polymer glasses. Results for a wide range

of multiaxial loading conditions, temperatures and potential parameters were consistent with the pressure-modified von Mises criterion. In this criterion, the driving force for shear is the deviatoric stress $\tau_{\text{dev}} = ((\sigma_1 - \sigma_2)^2 + (\sigma_2 - \sigma_3)^2 + (\sigma_3 - \sigma_1)^2)^{1/2} / 3$, where the σ_i are the three eigenvalues of the stress tensor. Rather than having a sudden onset at a finite strain, irrecoverable deformation was observed at arbitrarily small strains. The most robust definition of the yield stress was τ_{dev}^y , the peak value of the deviatoric stress as a function of strain. This quantity increases linearly with pressure in agreement with the pressure-modified von Mises criterion.

The results in ref. [2] were obtained for a single value of the strain rate. Here we focus on the effect of varying strain rate on the shear yield stress. The initially cubic simulation cell is expanded in one direction at a constant strain rate $\dot{\epsilon}_z = L_z^{-1}dL_z/dt$, and volume V is conserved by maintaining $L_x = L_y = \sqrt{V/L_z}$. Fig. 1 shows the deviatoric stress averaged over the entire simulation cell as a function of strain at three different strain rates. As can be seen, the behavior of the bead spring model (a) and the binary LJ glass (b) is qualitatively similar. These curves also closely resemble experimental stress-strain curves for e. g. polymeric glasses [5].

For all systems the initial response is nearly elastic, i.e. the stress rises almost linearly with strain. In the quasistatic limit, the initial slope gives the elastic modulus. Results for strain rates of $3 \times 10^{-4}\tau_{\text{LJ}}^{-1}$ and below collapse onto this quasistatic behavior. As the strain rate rises to $10^{-3}\tau_{\text{LJ}}^{-1}$ and beyond, the initial slope grows. The reason is that stress is no longer able to equilibrate across the system. It is well known that the elastic modulus of a heterogeneous system is over-estimated by applying a uniform strain (the Voight limit [22]). Our algorithm imposes a uniform strain at each step by rescaling the cell dimensions and particle coordinates and the resulting stress will be too high when the strain rate becomes too large. A rough estimate for the characteristic time for stress equilibration through the system is $L/c \sim 10\tau_{\text{LJ}}$, where c is the speed of sound. When the strain is stopped suddenly we find an exponential stress relaxation with a characteristic time $\sim 15\tau_{\text{LJ}}$. At a strain rate of $\dot{\epsilon}_i = 10^{-3}\tau_{\text{LJ}}^{-1}$, the time to reach a strain of 2% is $20\tau_{\text{LJ}}$ and becomes comparable to the above estimates. We conclude from Fig. 1 that the shear rate is slow enough to produce a quasistatic deformation for $\dot{\epsilon}_i < 10^{-3}\tau_{\text{LJ}}^{-1}$, but not at the highest shear rates.

As the strain increases, even the curves for lower strain rates split apart and saturate at different maximum heights τ_{dev}^y . The maxima are broad and centered at strains of about 6% in the binary LJ glass and 8% in the polymer. The fine structure on the curves corresponds to individual plastic yield events that are discussed further below. This structure decreases with increasing system size and temperature as the fraction of the system involved with typical events decreases. Results for larger systems were consistent with those shown here, but could

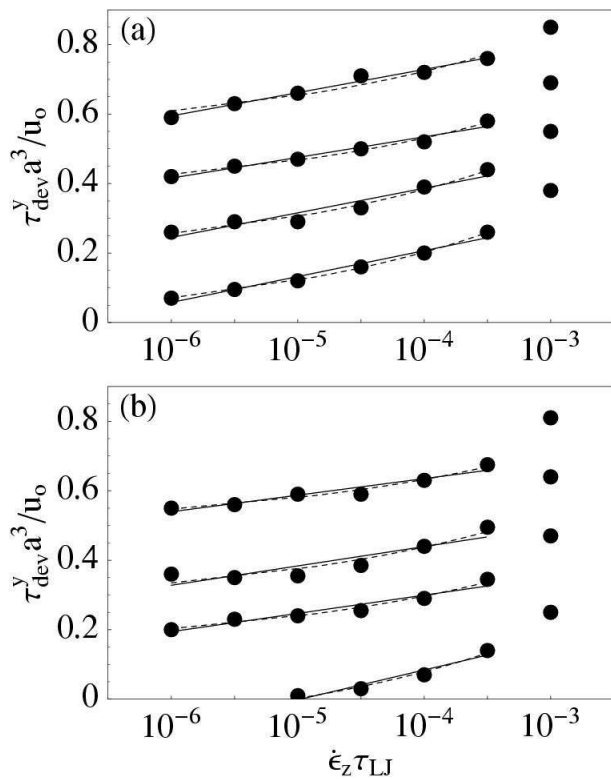


FIG. 2: Rate dependence of the maximum shear yield stress for (a) the polymer glass and (b) the 80/20 LJ glass. The temperature decreases from $T = 0.3 u_0/k_B$ (bottom data points) to $T = 0.01 u_0/k_B$ (top data points) with intermediate values of $T = 0.2 u_0/k_B$ and $T = 0.1 u_0/k_B$. Also shown are fits to a logarithmic rate dependence $\tau_{\text{dev}}^y = \tau_0 + s \ln \dot{\epsilon}$ (solid) and a power law $\tau_{\text{dev}}^y = \tau_0 + r \dot{\epsilon}^n$ (dashed) with $n = 0.2$. Fit values of s were (a) 0.028 ± 0.003 and (b) 0.022 ± 0.02 .

not be extended over as wide a range of shear rates and other parameters.

Fig. 2 summarizes values for τ_{dev}^y obtained from the maximum of curves such as those in Fig. 1 as a function of strain rate. Four different temperatures were studied, with the highest value, $T = 0.3 u_0/k_B$, close to T_g and $T = 0.01 u_0/k_B$ far away. This covers a much wider range than usually explored in experiments. For a given temperature and most strain rates, both models give nearly straight lines in a semilogarithmic plot. The salient observation that can be made in this figure is that all curves are nearly parallel, and temperature merely changes the offset value on the stress axis.

As suggested by the Eyring-model, an obvious way to describe the rate dependence is through a logarithmic fit of the form $\tau_{\text{dev}}^y = \tau_0 + s \ln \dot{\epsilon}$ (solid lines). The observation of parallel curves then implies a nearly constant prefactor s in front of the logarithm, and the variation with temperature is described by τ_0 . Often the rate dependence of the shear yield stress of complex materials is also described with a power-law added to a constant, i. e. $\tau_{\text{dev}}^y = \tau_0 + r \dot{\epsilon}^n$ (dashed lines). As can be seen in

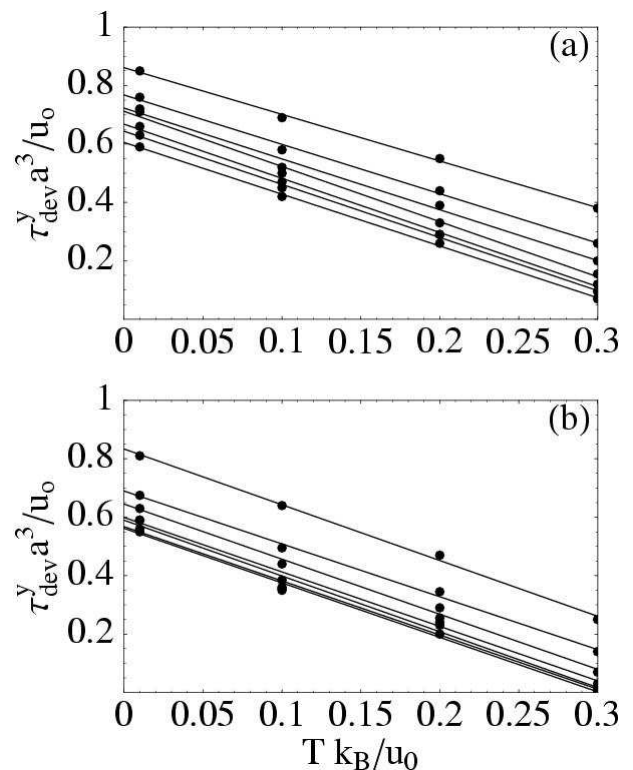


FIG. 3: Variation of the shear yield stress with temperature for (a) the polymer glass and (b) the 80/20 LJ glass. The rates vary between $10^{-3} \tau_{\text{LJ}}^{-1}$ and $10^{-6} \tau_{\text{LJ}}^{-1}$ as in Fig. 2 (from top to bottom). Linear fits to the data points for a given rate are also shown.

Fig. 2, such fits provide an equally good description of the data. Due to the small variations of τ_{dev}^y , a determination of the exponent n via best fits is very unreliable. Since the curves for different T are nearly parallel, there is no reason to expect n to vary. The curves in Fig. 2 are for $n = 0.2$, which gave the smallest variation of the prefactor r ($< 10\%$) with temperature, but other choices between 0.1 and 0.3 are also possible. Since $\tau_0 > 0$ for $T \leq 0.2 u_0/k_B$, the data is not consistent with a pure power law.

Neither functional form provides a good fit to results at the highest strain rate $10^{-3} \tau_{\text{LJ}}^{-1}$. We have already shown that the elastic behavior changes at this shear rate because stress can not equilibrate throughout the system. The plastic response will also be affected by the dynamics of stress distribution, and new behavior is expected to set in at this rate. Therefore, these points were not included in the fits shown in Fig. 2. Note that experiments are always at much lower strain rates, while most simulations of shear have been done at $\dot{\epsilon}_i = 10^{-5}$ to $10^{-1} \tau_{\text{LJ}}^{-1}$. A clear distinction between a logarithm and a power-law dependence would thus only be possible by measuring the yield stress at lower rates, but unfortunately the simulation time becomes prohibitively large.

The fact that the curves of Fig. 2 are parallel implies

that replotting the shear yield stress as a function of temperature also leads to parallel behavior. Fig. 3 shows that the trend of τ_{dev}^y with T is in fact linear, and the slope is nearly rate independent. The rate merely changes the offset value.

In order to investigate whether the rate dependence is in any way influenced by the methodology, we have expanded our studies and considered other model parameters, different thermostat methods and loading states. In particular, we obtained data analogous to that shown in Fig. 2 for a longer range of the Lennard-Jones potential $r_c = 2.2a$, Nosé-Hoover and Langevin thermostats with different rates, and uniaxial strain as opposed to the volume-conserving shear in Fig. 1. We also considered a system that was quenched into the glassy state 10 times faster than the other systems to investigate cooling rate effects. All these different situations show essentially the same robust scenario: the rate dependence is nearly independent of temperature with a constant offset that decreases linearly as T increases. The slope s is generally unaffected within the noise, but is roughly twice as large for uniaxial strain, and slightly larger for rapidly quenched initial states. Again, power-law fits could also be used to describe the data, and a fixed exponent suffices to describe all temperatures.

B. Steady shear

Most rheological measurements of soft glassy materials focus on the steady state stress and not on the initial transient maximum of the stress-strain curve. Thus it is interesting to compare the rate dependence for steady state shear to the above results. The steady state can not be studied with the entangled bead-spring model used above [35], because the shear stresses at accessible strain rates would soon break covalent bonds. However previous studies with short chains [23] and the binary system [7, 24, 25] show similar trends with decreasing T . At high T

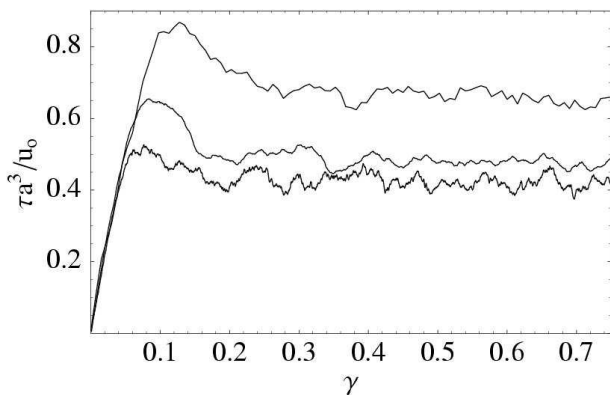


FIG. 4: Stress strain curves for simple shear of the binary LJ solid at $T = 0.1 u_0/k_B$ for three different shear rates $\dot{\gamma} = 0.01\tau_{\text{LJ}}^{-1}$, $\dot{\gamma} = 0.001\tau_{\text{LJ}}^{-1}$ and $\dot{\gamma} = 0.0001\tau_{\text{LJ}}^{-1}$ (top to bottom).

($\geq 0.7u_0/k_B$ for the binary system), Newtonian behavior is observed up to the highest practical shear rates. At lower temperatures, where the liquid is in a supercooled state, there is a crossover from Newtonian behavior at low rates to power law shear thinning $\sigma \sim \dot{\gamma}^n$ at high rates. The crossover rate goes to zero as T decreases to T_g , and at lower temperatures the shear stress is nearly independent of strain rate [23].

We focus here on the binary (80/20) LJ system at $T \leq 0.3u_0/k_B$, varying T from just above T_g to well below. As described in Section III, shear was imposed by confining the system between walls separated by h along the z -direction and translating one at a fixed speed v_x . Fig. 4 shows typical behavior of the stress as a function of the average shear strain γ . There is an initial maximum at $\gamma \sim 0.1$ that corresponds to the transient behavior studied in the previous section. The stress then decreases rapidly to a steady state plateau value. This strain softening becomes more pronounced with decreasing temperature.

The average value from the steady state region is plotted vs. shear rate in Fig. 5. At $T = 0.3u_0/k_B$ (lowest curve), the solid exhibits glassy behavior at high rates, but is Newtonian at lower rates, which indicates that the temperature is still above T_g . For all temperatures below T_g the curves are nearly parallel, as for the results for the transient maximum shear stress in Fig. 2. A logarithmic rate dependence may be fitted at small rates, but a power-law added to a constant clearly provides a much better fit over the whole range of rates. The fits for the temperatures $T \leq 0.2 u_0/k_B$ shown in Fig. 5 use $n = 0.3$, for which the prefactor r to the power-law deviates from unity by less than 10%. Our results for the glassy state are very similar to observations reported by Varnik *et al.* [26], who used the same model with a larger cutoff value $r_c = 2.5a$ for the LJ potential and only considered $T = 0.2u_0/k_B$.

The rate dependence of the steady shear stress is very similar to that of the yield stress (Fig. 2). In both cases, there is a rapid rise above the logarithmic fits at rates of $10^{-3}\tau_{\text{LJ}}$ and above. Although in Fig. 5 the system has had time to reach a steady state, one may wonder whether there is still a change in behavior near $\dot{\gamma} = 10^{-3}\tau_{\text{LJ}}^{-1}$. At higher rates the stress may not relax between the local yield events discussed below, leading to a more rapid rise in mean stress. The results were not extended to higher shear rates because the temperature in unthermostatted directions begins to rise slightly above the set temperature even at $\dot{\gamma} = 10^{-2}\tau_{\text{LJ}}^{-1}$.

A plot of the shear stress vs. rate as in Fig. 5 assumes that the local strain rate is equal to the average implied by v_x/h . Fig. 6 shows the velocity profile for two different temperatures and several different shear rates. The first few layers always move with the walls due to the strong coupling. At $T = 0.2 u_0/k_B$, the profile in the center region is homogeneous and here the assumption that v_s/h equals the shear rate is satisfied. However, at $T = 0.01 u_0/k_B$ shear is localized in the lower 60% of the

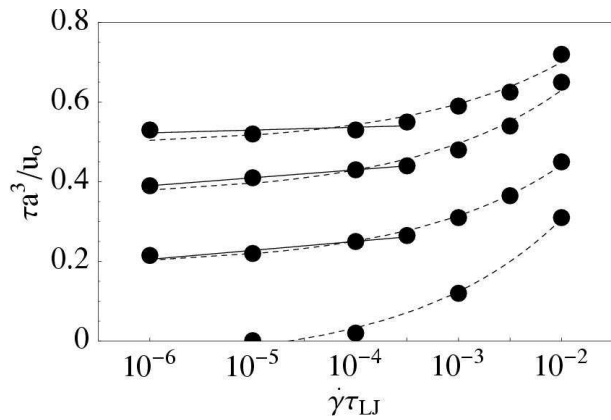


FIG. 5: Rate dependence of the steady state shear stress for the 80/20 LJ glass at 4 temperatures $T = 0.3 u_0/k_B$ (bottom), $T = 0.2 u_0/k_B$, $T = 0.1 u_0/k_B$, and $T = 0.01 u_0/k_B$ (top). Also shown are fits to a logarithmic rate dependence $\tau_{\text{dev}} = \tau_0 + s \ln \dot{\epsilon}$ (solid) and a power law $\tau_{\text{dev}} = \tau_0 + r \dot{\epsilon}^n$ (dashed), where $n = 0.3$ for all curves.

simulation cell, and the upper part of the glass moves at the constant wall speed. This is a clear indication of shear banding. The local shear rate is now larger than the average value, but since the change is only by about a factor of two, the data points in Fig. 4 are not dramatically affected.

In their simulations at $T = 0.2 u_0/k_B$, Varnik *et al.* [26] also found a transition from homogeneous flow to shear banding as the shear rate dropped below $10^{-3} \tau_{LJ}^{-1}$. In our simulations, shear is homogeneous at this temperature, but the shorter cutoff in our model implies a slightly lower T_g . The increasing amount of shear localization with decreasing temperature is consistent with a stress peak that becomes more pronounced as T is lowered (see Fig. 4). The region with negative slope on the stress-strain curve signals a mechanical instability and shear localization. This localization is inhibited in the simulations that were used to study the transient stress maximum, since they used periodic boundary conditions in all directions. Varnik *et al.* [26] noted that simulations with Lees-Edwards boundary conditions [27] also suppressed shear banding, but that the shear stresses obtained from simulations with walls and periodic boundary conditions are similar.

C. Analysis of the dynamics of the local stress distribution

One of the great advantages of molecular simulations is the ability to reach beyond a measurement of the macroscopic response function and in addition obtain information about the local dynamics and rearrangements in nonequilibrium situations. Such information is essential to construct a clear picture of the underlying microscopic processes.

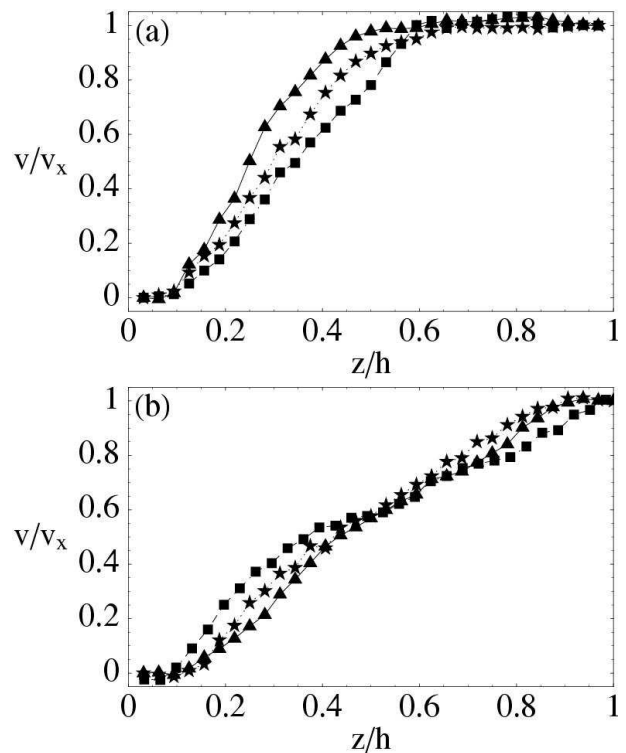


FIG. 6: Rescaled velocity profiles for 3 different shear rates $\dot{\gamma} = 10^{-3} \tau_{LJ}^{-1}$ (\blacktriangle), $\dot{\gamma} = 10^{-4} \tau_{LJ}^{-1}$ (\star), $\dot{\gamma} = 10^{-5} \tau_{LJ}^{-1}$ (\blacksquare) at (a) $T = 0.01 u_0/k_B$ and (b) $T = 0.2 u_0/k_B$. The velocities are rescaled by the wall velocity v_x and the positions by the total separation h of the walls.

Here, we follow this route by decomposing the total simulation cell into small volume elements of size $7 - 8a^3$ and measuring the local stress tensor in those regions. Since the density is close to $1a^{-3}$, these regions contain typically 7-8 particles. A particle number of that size should be sufficient to constitute a locally transforming region as envisioned in several of the theoretical models described in Section II. Some of the models suggested that local rearrangements replace thermal noise as the source for activation over barriers, which motivates a study of the stress changes experienced by local regions.

Our results for general stress states [2] have shown that the deviatoric shear stress τ_{dev} is the relevant stress tensor invariant that describes shear deformation. We therefore calculate the local change $\Delta\sigma_{ij}$ in the stress tensor in every volume element during a small time interval and then study the size distribution of changes in the scalar variable $\Delta\tau_{\text{dev}}$ calculated from $\Delta\sigma_{ij}$ (note that $\Delta\tau_{\text{dev}}$ is always positive, since it refers to the deviatoric stress of $\Delta\sigma_{ij}$). In general, one expects $\Delta\tau_{\text{dev}}$ to fluctuate even in the undriven case, and one should expect to find a stationary distribution of stress jumps over not too long timescales. Since the glass is out of equilibrium, it is by construction not stationary and will exhibit aging phenomena, etc. Such long timescales, however, are not ex-

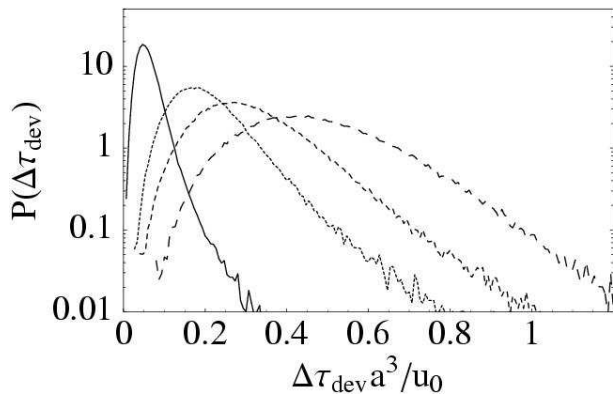


FIG. 7: Size distribution of jumps $\Delta\tau_{\text{dev}}$ for the *unstrained* binary LJ glass at four temperatures $T = 0.01u_0/k_B$ (solid line), $T = 0.1u_0/k_B$, $T = 0.2u_0/k_B$ and $T = 0.3u_0/k_B$ (long dashed line, T increases from left to right). $\Delta\tau_{\text{dev}}$ was calculated for a time difference of $7.5\tau_{\text{LJ}}$. The distributions are stationary over $\sim 10^5\tau_{\text{LJ}}$.

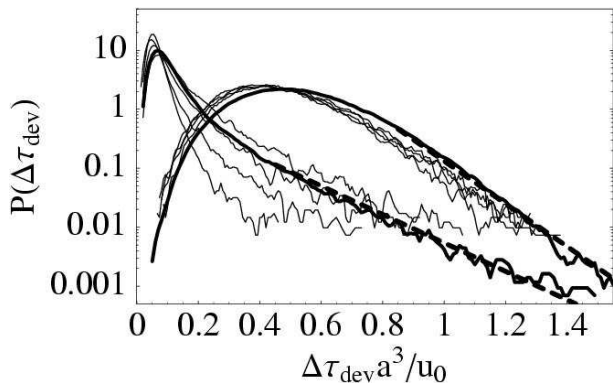


FIG. 8: Size distribution of jumps in τ_{dev} for the binary LJ glass *sheared* at $\dot{\gamma} = 10^{-4}\tau_{\text{LJ}}^{-1}$ for two temperatures $T = 0.01u_0/k_B$ and $T = 0.3u_0/k_B$. Different curves belong to strains of 0%, 2.5%, 4.5% and 7% (see Fig. 1). Also shown as thick solid lines are the steady state distributions at the same rate as well as exponential fits (dashed lines) to the tail of those distributions.

plored here.

Fig. 7 shows an example of such stationary distributions for four different temperatures. The jumps correspond to an average change in local deviatoric stress in small regions over a time difference of $7.5\tau_{\text{LJ}}$. The narrowest distribution is found at the lowest temperature $T = 0.01u_0/k_B$ and the distribution widens as the temperature increases to $T = 0.3u_0/k_B$. The cause for the stress jumps is obviously thermal motion of the particles, and only small excursions about their positions can occur in the glass (cage effect). The part of the distribution at small values of $\Delta\tau_{\text{dev}}$ can be fitted to a Gaussian, but deviations become visible at large values.

We are now able to determine how the distribution of

stress jumps in the undriven system changes when the system is macroscopically strained. Fig. 8 shows several distributions at the highest ($T = 0.3u_0/k_B$) and lowest ($T = 0.01u_0/k_B$) temperatures considered. $\Delta\tau_{\text{dev}}$ was calculated for the same time difference $7.5\tau_{\text{LJ}}$. For each temperature, four distributions are shown, which correspond to four different strains between zero and the maximum shear yield strain. Also shown for comparison are the distributions in steady shear.

Several observations can be made in this figure. Note first that at $T = 0.3u_0/k_B$, the unstrained distribution is not changed dramatically under external driving. Only the tail at large jumps gets modified. This temperature is above T_g and the shear rate is low enough that the deviation from Newtonian behavior is small. This is in sharp contrast to the situation at $T = 0.01u_0/k_B$, where strain produces a dramatic increase in the number of large jumps. The tail of the distribution can be fit to an exponential form $\exp(-\Delta\tau_{\text{dev}}/\tau_c)$ that extends to larger stresses as the strain increases to the peak in the stress-strain curve. The steady state stress results are close to those at a transient strain of 4.5%. The steady state probability curves decay with the characteristic stresses $\tau_c = 0.18u_0/a^3$ ($T = 0.01u_0/k_B$) and $\tau_c = 0.12u_0/a^3$ ($T = 0.3u_0/k_B$).

V. INTERPRETATION AND COMPARISON TO MODELS OF PLASTICITY

The above results for the strain rate dependence of shear yielding offer an opportunity to test the theoretical models described in Section II. The Eyring model Eq. (2) predicts a logarithmic dependence of τ_{dev}^y , and the prefactor s is given by $k_B T/V^*$. Since we found typical values of s between 0.02 and 0.03 for all temperatures, our result can only be reconciled with the Eyring model if one allows for huge variations of the “activation volume” V^* between $0.3a^3$ and $10a^3$. V^* is a phenomenological fit parameter, but is typically interpreted as a characteristic volume for a local shear event. It should then be at least of order the volume per particle, i.e. of order a^3 or larger. The implied linear change in V^* with T would also be inconsistent with the observed linear temperature dependence of τ_{dev}^y . From Eq. (2) the stress would vary as $E/V^* \sim E/T$, which is inconsistent with the data. Besides, the usefulness of the Eyring expression is reduced if V^* is allowed to be temperature dependent.

Modern theories offer a different interpretation of the rate dependence. Lemaître’s extension [4] of the STZ theory [3] to include free volume relaxation produces complex rate dependence that could describe our results. However, the issue of temperature dependence has not been addressed in this approach and we have not examined the issue of free volume relaxation here.

A pure power-law shear thinning behavior was predicted in the calculations of Berthier *et al.* [11]. Starting from very different considerations, these authors found

that the exponent n should have a generic value of $1/3$ at a transition temperature T_c . Below T_c , the exponent should in principle be temperature dependent, but their numerical results indicated only a very weak dependence. Both results are consistent with our findings near T_g , but not at lower temperatures where we find a constant plus power-law behavior.

Below the glass transition temperature, the SGR model [10] predicts such constant plus power-law behavior of the flow curve with an exponent of the form $1 - x$, where x is an effective noise temperature in units where the glass transition temperature $x_g = 1$. In steady shear, we found good agreement with this functional form and an exponent $n = 0.3 \pm 0.1$. The authors of the SGR model go to great length in providing an interpretation for x . They argue that in a sheared state, the energy for surmounting a barrier for rearrangement is not only provided by the thermal energy, but also by the energy released from rearrangements elsewhere in the material. This energy diffuses through the material and provides an effective thermal bath in a mean field sense. The energy released in such a rearrangement must therefore be of order of the typical yield energies, which implies that x should be of order unity. When the yield energies are much larger than typical thermal energies, x will be independent of the true thermodynamic temperature T . Our finding of an exponent independent of T could thus be rationalized in this framework.

Our analysis of the distribution of local stress jumps could lend additional support to the concepts behind the SGR model. Changes in the local deviatoric stress as shown in Fig. 8 can activate yield events. We found that the distribution of stress jumps could be fitted to an exponential distribution with a characteristic decay stress that varied less than 30% as T changed from $0.3 u_0/k_B$ to $0.01 u_0/k_B$. At small values of $\Delta\tau_{dev}$, the distribution retains the equilibrium form. This result suggests that the drive generates internal dynamics on a common scale despite very different thermodynamic temperatures and might provide a more microscopic justification of the background “effective noise temperature” proposed in the SGR model.

The shear energy released by a yielding local region should indeed trigger additional yield events at other locations in the material. However, the ensuing dynamics may be more complicated than suggested by mean-field approaches. Many models of material breakdown include load redistribution mechanisms. In fiber bundle models [28], for instance, one finds avalanche behavior that precedes total failure. The avalanche size distribution follows a power law. When shearing a material, however, a yielded region will typically reemerge with a different yield energy as assumed in the SGR model. In ref. [29], the simpler situation of an elastic network with random breaking thresholds of the links was subjected to an external drive. Damaged elements were replaced with new ones with a different breaking threshold. Power-law behavior in the size and duration of failure events was

found. Recent work on molecular [30] as well as simplified models [31] shows that load redistribution in the yielding glass mediated by elastic interactions between rearranging regions can lead to avalanche behavior.

VI. CONCLUSIONS

The (transient) maximum deviatoric shear stresses for two model glasses, binary LJ mixtures and polymers, were shown to exhibit strikingly similar trends with rate and temperature. The rate dependence was remarkably constant from $\sim T_g$ to temperatures 30 times lower. The entire flow curve shifted linearly to lower stress as T increased. At low rates, the rate dependence of the peak stress could be described by a logarithm or constant plus power-law, where the prefactor and/or exponent did not vary with temperature. A more rapid rise in stress was observed when strain rate was increased to $10^{-3}\tau_{LJ}^{-1}$. Deviations in the elastic response also set in at this strain rate, indicating that stress could not relax throughout the system. This is not surprising given that the time to strain to 1% is comparable to that of sound propagation back and forth across the system.

The stress for steady shear flow was calculated for the LJ mixture. Curves for different temperatures were also nearly parallel, shifting rigidly to lower stresses with increasing temperature. Below strain rates of $10^{-3}\tau_{LJ}$, the dependence of the flow stress on rate could be described by a logarithm. The entire flow curve could be fit by a constant plus power law with a temperature independent exponent $n = 0.3 \pm 0.1$. However, as for the transient stress, the stress begins to rise more rapidly at $10^{-3}\tau_{LJ}^{-1}$. It is interesting to ask whether the emergence of a power-law vs. logarithmic behavior is related to the overlap of shear rate and stress equilibration timescales. Although the system is in steady state, regions of a few atoms undergo a substantial yield event after of order 1% strain increments. At strain rates of $10^{-3}\tau_{LJ}^{-1}$ and above, the time between these yield events will be too short for stress relaxation in our system. This point should be kept in mind when comparing molecular simulations to experiments at lower strain rates.

The Eyring model was shown to be incompatible even with logarithmic fits to the shear stress at low rates. It predicts that the prefactor of the logarithm should scale as kT/V^* , while the observed prefactor is nearly independent of temperature. Fixing this discrepancy by requiring V^* to scale linearly with T leads to unphysically small values of V^* and is inconsistent with the linear drop in yield stress with temperature at a given rate. The Eyring model has been very helpful in analyzing experimental data, but typically over a narrow range of temperatures. It would be interesting to extend these measurements to very low temperatures and to higher shear rates. Note that typical room temperature experimental values for V^* in polymers correspond to 3 or 4 repeat units [8], which is of the same order as the values

we find at $T = 0.1$ or $0.2u_0/k_B$.

The insensitivity of the rate dependence to temperature changes indicates that thermal activation is not dominant at the rates studied. Analysis of the individual particle trajectories offers an explanation for this. Even in the limit of zero temperature we find that the trajectories are exponentially sensitive to changes in rate and other parameters. The system does not travel along a single path through the energy landscape at different rates, but gets deflected between many possible paths by small perturbations.

Both the STZ and SGR models describe complex dynamics in systems where temperature is unimportant. Instead, activation is due to another internal state variable, either v_f or x , that couples to the external drive via a feedback mechanism. The original STZ theory gives a simple linear rise in stress with rate above the yield stress [3]. However recent generalizations [4] can produce more complex rate dependence like that found here. The SGR model predicts a constant plus power-law behavior that is also consistent with our simulations and can account for a temperature independent exponent n . It remains to be seen whether the generating mechanism of structural disorder (SGR) or free volume dynamics (STZ) provides a more useful description of glassy dynamics.

An external drive introduces a new timescale into the problem that couples to the structural rearrangements. It will therefore modify the associated relaxation time scales and alter the unperturbed glassy dynamics, e.g to stop aging and induce rejuvenation [6]. At zero temperature, this timescale should be the only one present in the system, while other competing timescales will arise

at finite temperature. Associated with this timescale is the concept of an effective temperature [7, 32] that also appears in the SGR model. While this picture is clearly a useful starting point, the analysis of the jump distribution has shown that the internal dynamics of the flowing glassy solid is much more intricate and strongly calls for extensions of analytical models beyond mean-field concepts. Such a treatment should describe more accurately the load redistribution mechanisms and the propagation of released shear energy on a microscopic level. A preliminary analysis has shown that local plastic events occur in avalanches over a wide range of length and time scales.

Finally, we note that the above analytic models of glassy rheology and viscoplasticity are all scalar models that cannot describe self-organization on larger length scales such as shear bands. Tensorial versions of the STZ theory are being discussed to address banding and necking [33]. These are promising approaches that should continue to benefit from insight gained from molecular simulations, in particular the load redistribution mechanisms of shear yielding zones.

VII. ACKNOWLEDGEMENTS

We thank J. S. Langer and M. L. Falk for useful discussions. Financial support from the Semiconductor Research Corporation (SRC) and NSF grant No. DMR0083286 is gratefully acknowledged. The simulations were performed with *LAMMPS 2001* [34], a molecular dynamics package developed by Sandia National Laboratories.

-
- [1] R. G. Larson, *The structure and rheology of complex fluids* (Oxford University Press, New York 1999).
- [2] J. Rottler, M. O. Robbins, Phys. Rev. E **64**, 051801 (2001).
- [3] M. L. Falk and J. S. Langer, Phys. Rev. E **57**, 1971 (1998), M. L. Falk and J. S. Langer, M. R. S. Bulletin **25**, 40 (2000).
- [4] A. Lemaitre, Phys. Rev. Lett. **89**, 195503 (2002) and cond-mat/0206260.
- [5] O. A. Hasan and M. C. Boyce, Polymer Eng. and Sci. **35**, 331 (1995).
- [6] A. J. Liu and S. R. Nagel (Eds.), *Jamming and Rheology*, (Taylor & Francis, London, 2001)
- [7] J. L. Barrat, L. Berthier, Phys. Rev. E **63**, 012503 (2000), L. Berthier, J. L. Barrat, Phys. Rev. Lett **89**, 095702 (2002).
- [8] I. M. Ward, *Mechanical Properties of Solid Polymers* (John Wiley & Sons, New York 1983).
- [9] H. Eyring, J. Chem. Phys. **4**, 283 (1936).
- [10] P. Sollich, F. Lequeux, P. Hébraud, M. E. Cates, Phys. Rev. Lett. **78**, 2020 (1997), P. Sollich, Phys. Rev. E **58**, 738 (1998), S. Fielding, P. Sollich, M. E. Cates, J. Rheol. **44** 323 (2000).
- [11] L. Berthier, J.-L. Barrat, J. Kurchan, Phys. Rev. B **61**, 5464 (2000).
- [12] C. Monthus and J.-P. Bouchaud, J. Phys. A: Math. Gen. **29**, 3847 (1996).
- [13] T_c refers to a dynamical transition temperature, where the relaxation time in the model diverges as a power law.
- [14] K. Kremer and G. S. Grest, J. Chem. Phys. **92** 5057 (1990).
- [15] M. Pütz, K. Kremer, G. S. Grest, Europhys. Lett. **49**, 735 (2000).
- [16] W. Kob and H. C. Andersen, Phys. Rev. E **51**, 4626 (1995), Phys. Rev. E **52**, 4134 (1995).
- [17] W. Kob and J.-L. Barrat, Phys. Rev. Lett. **78**, 4581 (1997).
- [18] W. Kob, C. Donati, S. J. Plimpton, P. H. Poole, and S. C. Glotzer, Phys. Rev. Lett. **79**, 2827 (1997).
- [19] C. Bennemann, W. Paul, K. Binder and B. Dünweg, Phys. Rev. E **57** 843 (1998).
- [20] M. P. Allen, D. J. Tildesley, *Computer Simulations of Liquids* (Oxford University Press, Oxford 1987).
- [21] P. A. Thompson and M. O. Robbins, Phys. Rev. A **41**, 6830 (1990).
- [22] W. Voight, Lehrbuch der Kristallphysik (Teubner, Leipzig, 1928).
- [23] A. R. C. Baljon and M. O. Robbins, Science **271**, 482

- (1996); A. R. C. Baljon and M. O. Robbins, “Stick-Slip Motion, Transient Behavior, and Memory in Confined Films,” in *Micro/Nanotribology and its Applications*, edited by B. Bhushan (Kluwer, Amsterdam, 1997) pp. 533-553.
- [24] R. Yamamoto and A. Onuki, Phys. Rev. E **58**, 3515 (1998).
- [25] D. J. Lacks, Phys. Rev. Lett. **87**, 225502 (2001).
- [26] F. Varnik, L. Bocquet, J.-L. Barrat, L. Berthier, Phys. Rev. Lett. **90**, 095702 (2003).
- [27] L. Berthier and J.-L. Barrat, J. Chem. Phys. **116**, 6228 (2002).
- [28] M. Kloster, A. Hansen, P. C. Hemmer, Phys. Rev. E **56**, 2615 (1997)
- [29] S. Zapperi, A. Vespignani, H. E. Stanley, Nature **388**, 658 (1997)
- [30] G. Gagnon, J. Patton, and D. J. Lacks, Phys. Rev. E **64**, 051508 (2001)
- [31] J.-C. Baret, D. Vandembroucq, and S. Roux, e-print cond-mat/0206523.
- [32] Ian K. Ono, Corey S. O’Hern, D. J. Durian, Stephen A. Langer, Andrea J. Liu, and Sidney R. Nagel, Phys. Rev. Lett. **89**, 095703 (2002).
- [33] J. S. Langer, Phys. Rev. E **64**, 011504 (2001), L. O. Eastgate, J. S. Langer, L. Pechenik, e-print cond-mat/0206363.
- [34] <http://www.cs.sandia.gov/~sjplimp/lammps.html>.
- [35] The bead-spring model could be used when the chain length is very short.